land

MDPI

Article

Active Floodplain Sedimentation Dynamics in the Upper Tisza Region, Hungary, After River Regulation

Róbert Vass [1], Azin Rooien [1], Péter Czomba [2], Dávid Balázs [1], Beáta Babka [1] and György Szabó [1,*]

[1] Department of Landscape Protection and Environmental Geography, Institute of Earth Sciences, Faculty of Science and Technology, University of Debrecen, 4032 Debrecen, Hungary; vass.robert@science.unideb.hu (R.V.); azin.rooien@science.unideb.hu (A.R.); balazs.david@science.unideb.hu (D.B.); babkabeata@science.unideb.hu (B.B.)

[2] Institute of Environmental and Natural Sciences, University of Nyíregyháza, 4400 Nyíregyháza, Hungary; czomba.peter@nye.hu

* Correspondence: szabo.gyorgy@science.unideb.hu; Tel.: +36-208021822

Abstract

River regulation and embankment construction have fundamentally altered the hydrological relationships and sediment accumulation dynamics of floodplains worldwide. This study examines the accumulation conditions in the Upper Tisza (Hungary) floodplain, focusing on the different surface development conditions of oxbow lakes and fossil natural levees following human intervention. During the study, we integrated high resolution LIDAR terrain models with detailed sedimentological analyses (grain size composition, pH, EC, OC, $CaCO_3$). We used multivariate statistical methods (principal component and cluster analysis) to separate soil formation processes and sediment accumulation. Based on our results, we identified sharp sedimentological boundaries indicating artificial meander cutting (1852). We demonstrated that the cut meanders function as sediment traps, where the accumulation of fine grained sediments is significantly faster (>0.34 cm/year) than on the higher elevation natural levees (0.1 cm/year). Statistical analysis identified five distinct sedimentation environments, successfully separating recent soil levels from river sediments. These results provide an important basis for the complex management of floodplains, such as flood protection, water retention, and habitat management planning.

Keywords: active floodplain; sedimentation; river regulation; oxbow lake; natural levee; cluster analysis; PCA; Upper Tisza

Academic Editor: Nick B. Comerford

Received: 16 January 2026
Revised: 6 February 2026
Accepted: 11 February 2026
Published: 13 February 2026

1. Introduction

Alluvial plains are among the most actively developing areas [1–3]. This is particularly true of active floodplains, where the construction of embankments, river regulation, and the resulting changes in hydrological conditions have a significant impact on the process of sediment accumulation [2,4]. Sediment formation dynamics in floodplains is a complex process influenced by a number of factors, primarily the discharge of the river, the frequency and intensity of floods, the distance from the riverbed, and the topography of the floodplain.

Due to the embankments, rivers are unable to form the surface to the same extent as before river regulation, because they are forced to deposit their sediment in a narrow strip of the floodplain. This phenomenon leads to increased deposition in floodplains, which poses a significant flood risk. Sedimentation on the protected side of the embankment is only possible during extreme floods involving embankment breaches or floods that overflow the crest of the embankment [5].

It is very important to understand the dynamics of floodplain sedimentation, because only with this knowledge can the safe flow of floods be guaranteed in the long term, and it also fundamentally influences the possibilities for the utilization of floodplain areas. The dynamics of sediment accumulation can be studied using a number of methods [6–9].

If we only want to examine a shorter period, such as the specific impact of a flood event, the thickness of the fresh sediment layer can be easily determined after the flood has receded. If we want to examine a period spanning several decades or even centuries, we need to analyze the vertical profile of the accumulated sediment layer [7,10]. In the case of collected sediment samples, the grain composition, organic matter and heavy metal content, and magnetic susceptibility of the layers must be examined in the laboratory.

The average accumulation rate can be determined using marker layers identified in the profiles (e.g., known flood sediments, known anthropogenic pollutants) [7,11–15]. Radioactive isotopes can also be used to study accumulation processes. The radioisotope ^{137}Cs binds very well to soil particles, making it ideal for long-term (decades) estimates of sediment accumulation or soil loss [14–20].

The accumulation of floodplain and active floodplain areas is often determined using a marker layer associated with a heavy metal [21–24]. In most cases, the formation of heavy metal marker layers can be attributed to an accident that occurred at a specific point in time. One such event was the cyanide and heavy metal pollution of the Tisza River in 2000, after which there was a sharp increase in the number of studies conducted in the Tisza active floodplain [1,25–29].

The vertical and horizontal patterns of the grain composition of sediments alone provide a wealth of information about their sedimentation conditions and the energy conditions of the floodplain [30]. Walling et al. [30] measured the dominance of the sand fraction in the coastal strip of the River Ouse in the United Kingdom at a distance of 20–40 m from the riverbed, with finer fractions prevailing further away. One of the least equipment-intensive tests is the identification of a sedimentological marker layer of known age. This mainly occurs during river regulation projects involving riverbed relocation [1,28,29,31], or from changes in land use that increase erosion in the upper reaches of the river, or from newly initiated anthropogenic activities, which result in the accumulation of coarser-grained sediments with lower organic matter content [32,33].

The examination of the organic carbon (OC) content of floodplain sediments can contribute to the reconstruction of surface development. Floodplain sediment studies conducted on rivers in the Rocky and Cascade Mountains in the USA have shown that the organic matter content of individual profiles generally decreases from the surface, but peaks at deeper levels can also occur in rare cases [9].

The amount of OC depends on the age of the surface, because older surfaces have longer vegetation cover, allowing more organic matter to form and accumulate [34,35].

The pH values of floodplain sediments are crucial because they directly influence the rate of chemical weathering, mineral transformation, and organic matter decomposition, and thus the stability and long-term preservation of the sediments [36]. In addition to local geological conditions, the pH conditions of floodplain sediments are primarily influenced by changes in the mineralization process and oxidation-reduction conditions of the organic matter content of the sediment [9].

The calcium carbonate ($CaCO_3$) content of floodplain sediments is important because it strongly influences pH and thus indirectly influences weathering processes, mineral transformation, and the preservation of organic matter in the sediment sequence.

The examination of electrical conductivity (EC) is important in terms of floodplain sediment accumulation because it is a direct indicator of the amount of salts and ions dissolved in pore water, and thus of the long-term balance between water coverage, evaporation,

and infiltration. Changes in EC during and after flood waves clearly show how much dissolved material (e.g., carbonates, sulphates, chlorides, nutrient ions) is transported and accumulated in floodplains [37].

The extent of floodplain filling can also be determined using a database created by remote sensing or other digital methods. One such method uses largescale contour maps to determine the extent of accumulation using a digital terrain model (DTM) created from digitized contour lines [29,38–40]. Gábris et al. [38] measured a sedimentation rate of 0.5 cm/year in the Middle Tisza region. The method is based on comparing the average heights of areas inside and outside the embankment. The measurement is based on the principle that prior to the construction of the embankment, the two areas were characterized by nearly identical elevation conditions, and if higher elevation values are obtained in the floodplain, this is the result of accumulation limited to a narrow area. In Hungary, morphological changes along the entire length of the Tisza active floodplain are examined along so-called VO (Hydrographic Department) registration cross-sections marked by fixed elevation points [4]. Measurements have been carried out at VO cross-sections since 1890, typically every 30–40 years, using a theodolite. Between 1976 and 2014, a total of 69 sections were examined in the upper section between the towns of Tokaj and Tiszabecs. In 42 cases, the accumulation of active floodplain between 10 and 150 cm was measured, no change was observed in 11 sections, and erosion of 10–30 cm was measured in 16 sections. A total of five VO sections showed accumulation greater than 50 cm. The average sedimentation rate of 69 VO was 18 cm, which corresponds to a specific sedimentation rate of 0.47 cm/year [4].

The primary objective of our study is to conduct a complex assessment of the landscape-forming effects of river regulation in the Upper Tisza floodplain. Our aim is to explore how anthropogenic interventions have influenced the further development of geomorphological forms. Our goal is to reconstruct the development of active floodplain surfaces by examining certain physical and chemical parameters of sediments, supplemented by topographic assessment. The novelty of the research means that, without the use of costly and therefore not necessarily widely available radioisotope and heavy metal tests, we attempted to determine the dynamics of sediment accumulation in the floodplain by statistical analysis of the physical (grain composition) and some easily determinable chemical properties of the sediments. Our aim is to determine the extent of accumulation in the active floodplain, as this is essential for flood protection management, nature conservation management plans, agricultural land use, and the rehabilitation of oxbow lakes.

Therefore, in our study, we attempt to answer the following questions by examining oxbow lakes and fossil natural levees in a floodplain section of the Tisza River in Hungary:

- Is there a relationship between the elevation, shape, and date of inactivation of individual floodplain features (oxbow lakes, fossil natural levees)?
- Can the sharp sedimentological imprint of river regulation be identified in the stratigraphic sequences, which could serve as a basis for determining the extent of alluvial sedimentation rate?
- To what extent can recent soil formation and sediment accumulation processes be distinguished using multivariate statistical methods (PCA, Cluster analysis), and how do the results help to delineate different sedimentary environments?

2. Materials and Methods

2.1. Study Area

The study area is located in Northeastern Hungary, in the floodplain of the Tisza River. The Tisza is the largest tributary of the Danube (catchment area: 157,186 km^2) and the most significant watercourse in the eastern part of the Hungarian Great Plain. The middle section of the Tisza River enters Hungary. The studied oxbow lakes and natural

levees are located on the border of the villages of Gyüre and Tiszaszalka, on the eastern edge of the Bereg alluvial floodplain (Figure 1). Here, the Tisza follows the north–south Kraszna tectonic line, which separates the Bereg Plain from the elevated Nyírség alluvial fan covered with blown sand formations. In the wider environment of the section under investigation, about two dozen overdeveloped meanders were cut through during river regulation works starting in the mid-19th century. As a result, the length between the water gauges above (Vásárosnamény 684.45 km, 101.98 m asl) and below (Lónya 650.75 km, 99.52 m asl) the sample area decreased from 55.8 km to 33.7 km, a reduction of 40%, while the stream gradient increased from 4.4 cm/km to 7.3 cm/km [41].

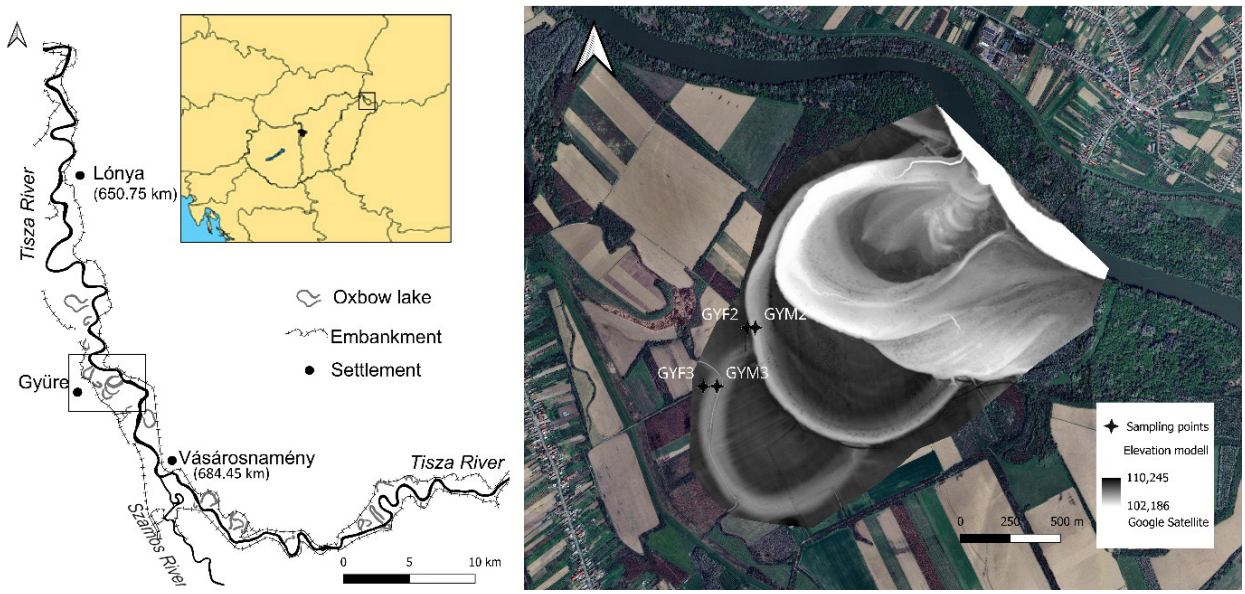

Figure 1. Location of the Gyüre floodplain sample area with sampling points.

In addition to river regulation, flood protection embankments were built at distances of typically 500–3000 m from each other, which also enclose the most of cut meanders. The Tisza River basin covers an area of 29,055 km^2 up to the mouth of the Szamos river in Vásárosnamény.

The river's watershed is influenced by oceanic, continental and mediterranean climate zones, therefore floods can be expected in three periods within a year. During March and April, floods caused by snowmelt may occur, while at the end of spring and beginning of summer, cyclones arriving from the Atlantic Ocean may cause flooding. Due to cyclonic activity arriving from the Mediterranean region in autumn, floods are also common in November and December [42].

Based on daily water level data from 1901 to 2013 at the water gauge located in the village of Tivadar, about 30 km above the study area (705.7 km, 105.4 m asl), annual maximum water levels show an increasing trend [43]. Partial flooding of the active floodplain (109 m asl) occurred in 98 of the 113 years, with an average water coverage of 9 days/year, while flooding with complete inundation (110.2 m asl) occurred in 54 years, with an average water coverage of 4 days/year [43]. The average water discharge at Vásárosnamény is 352 m^3/s, the minimum is 43 m^3/s, and the maximum discharge is 3702 m^3/s. The amount of suspended sediment transported at Vásárosnamény is 0.9 million m^3/year. The average grain diameter of bottom sediment samples taken at four cross-sections along a 6 km section of the river in the study area is 0.52 mm [44].

Measurements made between 1991 and 2013 in a river section approximately 20 km upstream of our sample area show that floods causing partial inundation of the floodplain have an average suspended sediment load of 550 g/m^3, while floods causing complete

inundation have an average load of 1517 g/m^3 [43]. The author concluded that higher water levels are also associated with more significant accumulation activity.

The average width of the Upper Tisza floodplain is 500–3500 m. In the study area, this value is 1600–3000 m. The reason for this is that three generations of oxbow lakes run parallel to each other here (Figure 1).

In our current work, we present the study of the two older oxbow lakes, designated GYM3 and GYM2 (Figure 1). In addition to the oxbow lakes, we also examined the sediments of the natural levees along their convex curves, marked GYF3 and GYF2.

A significant part of the sample area is used for ploughing, which affects the river banks. In these areas, the top 40 cm layer of soil is constantly being disturbed. Therefore, the natural levee sampling points were selected where ploughing is not carried out, these are areas of shelter belts and floodplain forests that have existed for several decades. We tried to establish the oxbow lake profiles in the immediate vicinity of the natural levee profiles.

The date of the meander cutoff of the oldest oxbow lake, GYM3, is unknown, but it must have happened before 1785, as it was already inactive on the first military survey map recorded in that year. The remaining length of the dead-end riverbed is 1.5 km, its width is 130–140 m, there is no permanent water cover, and the bank is difficult to identify due to its erosion. The elevation of the GYM3 profile is 106.1 m above sea level and is situated at 48°10′28.69″ N, 22°17′05.70″ E (WGS84). An artificial drainage channel 1.5 m wide and 1 m deep runs along the center line of the oxbow lake. The natural levee of the riverbank (GYF3) accompanying the oxbow lake surface rises about 1.5–2.5 m above the deepest level of meander, and the GYF3 profile is 108.6 m above sea level, situated at 48°10′29.57″ N, 22°17′03.45″ E (WGS84). A visual inspection of the terrain also clearly shows that the oxbow lake has been significantly deposited. The younger GYM2 oxbow lake, cut off during river regulation in 1852, is 2.17 km long and 90–110 m wide. There is no permanent water cover in this meander either; the GYM2 profile is 104.4 m above sea level and situated at 48°10′38.76″ N, 22°17′15.41″ E (WGS84). The concave bank of the natural levee is steep with a level difference of 3.5–5 m between the two forms and an elevation of GYF2; it is 109.3 m above sea level and situated at 48°10′38.45″ N, 22°17′13.75″ E (WGS84).

2.2. Methods

The sampling area was selected using Google Earth software and during field surveys A LiDAR-based terrain model with a resolution of five elevation points/m^2 was also used to accurately identify the forms. The terrain analysis was performed using Global Mapper 25.0 64-bit (Hallowell, ME, USA) and QGIS Destkop 3.28.15 Firenze software. To determine the exact elevation of the oxbow lakes and accompanying natural levees, we recorded cross-sections covering both the natural levees and oxbow lakes at 50–100 m intervals on the LiDAR-based terrain model in Global Mapper software. We calculated the average from the minimum and maximum values read from these.

Sampling took place in the autumn of 2023. We tried to designate sampling sections in undisturbed areas. In the case of oxbow lakes, we took samples at least 20 m away from the bank to avoid the effects of bank erosion. We collected 1000 g sediment samples from the wall of the sections at 2 cm intervals from the surface. In the case of natural levees, we collected samples to a depth of 100 cm, from the GYM3 oxbow lake to a depth of 120 cm, and from the GYM2 oxbow lake to a depth of 130 cm. A total of 225 samples were delivered to the laboratory of the Institute of Earth Sciences at the University of Debrecen.

The soil samples dried at 40 °C were pulverized, and the grain composition of the prepared samples was determined by sieving for fractions coarser than 0.2 mm, while further sedimentological examination of fractions smaller than 0.2 mm was performed using the Köhn pipette method in accordance with MSZ-08-0205-1978 [45].

We used the Miháltz scale to classify the samples according to grain size. We separated the following grain fractions: coarse and medium grained sand (2–0.2 mm), small grained sand (0.2–0.1 mm), fine grained sand (0.1–0.05 mm), coarse silt (0.05–0.02 mm), fine silt (0.02–0.002 mm), clay (<0.002 mm).

The chemical properties of the sediment were determined electrochemically using a WTX pH 340 measuring device in a 1:2.5 ratio of distilled water and potassium chloride suspension according to standard MSZ-08-0206/2-1978 [46].

The $CaCO_3$ content of the sediment was determined using a Scheibler calcimeter according to standard MSZ-08-0206/2-1978 [47], and the organic carbon (OC) content was determined using Tyurin's method according to standard MSZ-08-0210-1977 [48].

The electrical conductivity of the sediment was determined according to standard MSZ 21470–2:1981 [47].

The data were recorded in MS Excel software, and statistical analyses were performed using IBM SPSS 22 software. The distribution of the physical and chemical soil parameters examined was characterized by basic statistical indicators for individual section. The normality of the data was tested using the Shapiro–Wilk test. Since most variables did not show a normal distribution, non-parametric methods were used for further analysis. Spearman's rank correlation coefficients were calculated to explore the relationships between sediment parameters.

Principal component analysis (PCA) was performed with standardized variables to reduce the dimensionality of the data and reveal the main environmental gradients. The first two principal components were interpreted based on the loadings of the variables, and the distribution of the samples was plotted in PC1-PC2 space.

Hierarchical cluster analysis was used to group the samples based on their multivariate similarity. The variables included in the analysis were pH (H_2O and KCl), EC, $CaCO_3$ content, OC, and grain size composition. The variables were standardized using Z-score transformation. To determine the optimal number of clusters, we performed Ward's hierarchical clustering using Squared Euclidean distance. Based on the dendrogram and the elbow method, 5 clusters proved to be optimal. The final clustering was performed using the K-means method (N = 222 samples). The significance of the differences between the clusters was tested using one-way analysis of variance (ANOVA), and then cluster membership was represented in the depth profiles of the sections in order to interpret the sedimentation and soil formation patterns.

3. Results

3.1. Evaluation of the Terrain

Based on 18 cross-sections taken at equal distances from the GYM3 and GYF3 form complexes, it can be established that the average height of the natural levee is 108.78 m, the average level of the deepest points of the oxbow lake is 106.34 m, and the difference between them is 241 cm. Based on 23 cross-sections taken at the younger GYM2 oxbow lake, the ridge of the natural levee is 109.15 m, the average level of the deepest part of the oxbow lake is 104.75 m, and the difference in level here is 440 cm (Figure 2).

3.2. Physicochemical Characteristics of Sediments in Certain Geomorphological Forms

During the statistical evaluation, we first determined the basic statistical indicators of the examined parameters for each layer of individual floodplain form (Table 1).

Table 1. Basic statistical indicators of sediments of individual geomorphological forms (GYF2, GYF3: natural levee, GYM2, GYM3: oxbow lake).

Profile	Parameters	N	Minimum	Maximum	Mean	Std. Deviation	Variance
GYF2	pH (H_2O)	50	5.36	6.01	5.72	0.15	0.02
	pH (KCl)	50	4.22	5.47	4.91	0.41	0.17
	EC	50	53.60	325.00	105.79	56.87	3234.74
	$CaCO_3$	50	3.79	8.96	6.07	0.99	0.99
	OC	50	0.38	7.65	1.93	1.23	1.51
	Coarse and medium grained sand (2–0.2 mm)	50	0.00	0.00	0.00	0.00	0.00
	Small grained sand (0.2–0.1 mm)	50	4.40	36.50	14.06	6.56	43.07
	Fine grained sand (0.1–0.05 mm)	50	4.90	40.50	22.14	10.20	104.04
	Coarse silt (0.05–0.02 mm)	50	17.50	25.90	21.54	2.34	5.50
	Fine silt (0.02–0.002 mm)	50	19.60	58.20	31.90	11.21	125.61
	Clay (<0.002 mm)	50	7.20	18.00	10.35	2.24	5.04
GYF3	pH (H_2O)	50	5.01	6.53	5.88	0.42	0.18
	pH (KCl)	50	3.96	4.65	4.25	0.17	0.03
	EC	50	61.70	229.00	102.13	30.42	925.26
	$CaCO_3$	50	2.19	7.79	4.49	1.20	1.45
	OC	48	0.10	10.09	2.80	2.25	5.06
	Coarse and medium grained sand (2–0.2 mm)	50	0.00	0.70	0.12	0.18	0.03
	Small grained sand (0.2–0.1 mm)	50	0.10	11.70	4.36	2.62	6.84
	Fine grained sand (0.1–0.05 mm)	50	3.80	10.10	7.41	1.83	3.34
	Coarse silt (0.05–0.02 mm)	50	9.50	20.30	14.83	2.10	4.40
	Fine silt (0.02–0.002 mm)	50	37.90	56.80	47.60	5.64	31.78
	Clay (<0.002 mm)	50	14.50	34.80	25.67	4.91	24.09
GYM2	pH (H_2O)	65	5.13	8.00	7.03	0.88	0.78
	pH (KCl)	65	4.06	6.96	5.86	0.89	0.79
	EC	65	156.20	473.00	255.33	59.29	3515.35
	$CaCO_3$	65	3.38	11.81	6.74	1.12	1.26
	OC	65	0.92	7.22	2.02	1.11	1.24
	Coarse and medium grained sand (2–0.2 mm)	65	0.00	0.00	0.00	0.00	0.00
	Small grained sand (0.2–0.1 mm)	64	0.10	5.60	2.20	1.48	2.20
	Fine grained sand (0.1–0.05 mm)	65	0.90	9.00	4.13	1.94	3.77
	Coarse silt (0.05–0.02 mm)	65	2.00	24.90	9.57	4.98	24.83
	Fine silt (0.02–0.002 mm)	65	46.90	64.20	55.73	3.71	13.78
	Clay (<0.002 mm)	65	15.60	37.50	28.41	5.60	31.40
GYM3	pH (H_2O)	60	6.15	7.66	6.92	0.44	0.19
	pH (KCl)	60	5.17	6.65	5.73	0.43	0.18
	EC	60	91.40	697.00	201.91	98.87	9774.47
	$CaCO_3$	60	1.40	7.47	5.13	1.33	1.77
	OC	60	1.27	6.21	2.34	0.89	0.79
	Coarse and medium grained sand (2–0.2 mm)	60	0.00	0.00	0.00	0.00	0.00
	Small grained sand (0.2–0.1 mm)	60	0.10	8.20	3.38	1.50	2.26
	Fine grained sand (0.1–0.05 mm)	60	1.00	14.20	5.60	3.02	9.12
	Coarse silt (0.05–0.02 mm)	60	5.20	33.50	16.22	7.23	52.25
	Fine silt (0.02–0.002 mm)	60	38.20	57.00	50.38	4.13	17.08
	Clay (<0.002 mm)	60	13.80	40.40	24.42	7.36	54.23

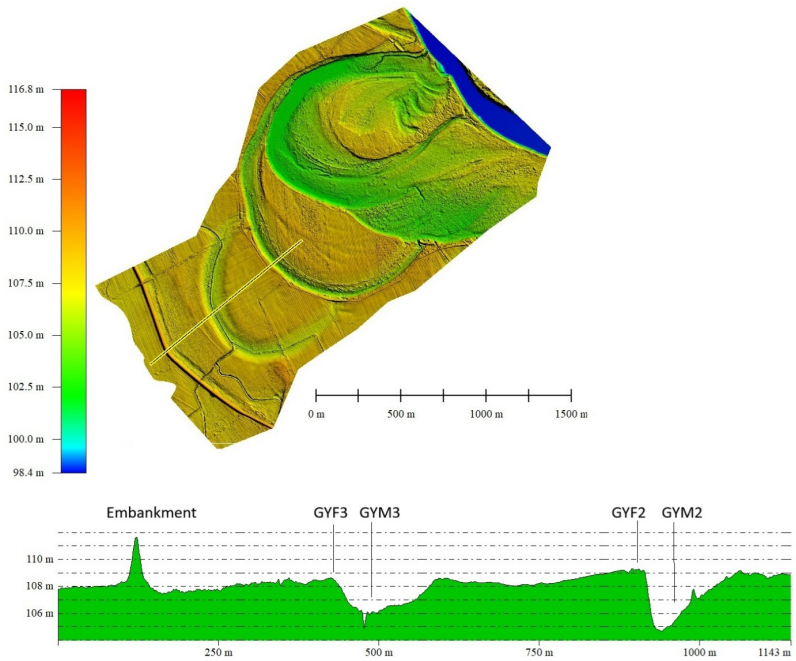

Figure 2. LiDAR-based terrain model and cross-section of the sample area.

When comparing samples from natural levee with samples from oxbow lakes, significant differences can be observed in some parameters. The pH (H_2O) values and the pH (KCl) values were significantly lower in the natural levees than in the two oxbow lakes studied (Figure 3).

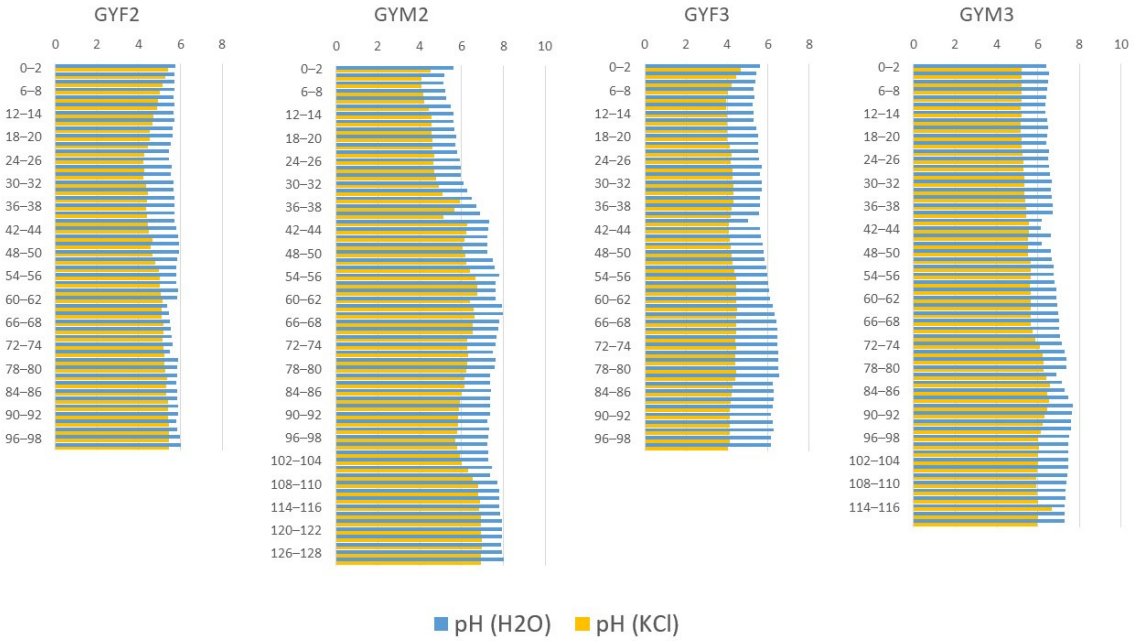

Figure 3. pH (H_2O) and pH (KCL) values of sediment layers in individual floodplain forms.

These results are consistent with the $CaCO_3$ content, as the average $CaCO_3$ concentration was lower in the GYF2 natural levee samples (6.07%) than in the GYM2 oxbow lake (6.74%), and the average of the GYF3 natural levee samples (4.49%) also falls short of the average value of 5.13% in the GYM3 oxbow lake (Figure 4). However, it should be noted that these differences are not significant, so pH values do not primarily depend on $CaCO_3$ content.

Figure 4. $CaCO_3$ content of sediment layers in different floodplain forms.

We did not observe any significant differences in the OC content of the sections. In all sections, the surface layers were richest in OC, especially in the case of the GYF3

natural levee, but the presence of OC was also detectable in the lower layers of the sections, although to a lesser extent (Figure 5). The most significant decrease was observed in the section of the oldest (GYF3) natural levee, where we measured values mostly below 1% in the lower layers of the section, while the OC content was much more uniform in the oxbow lakes, with values typically ranging between 1.5 and 2% in samples below 40 cm.

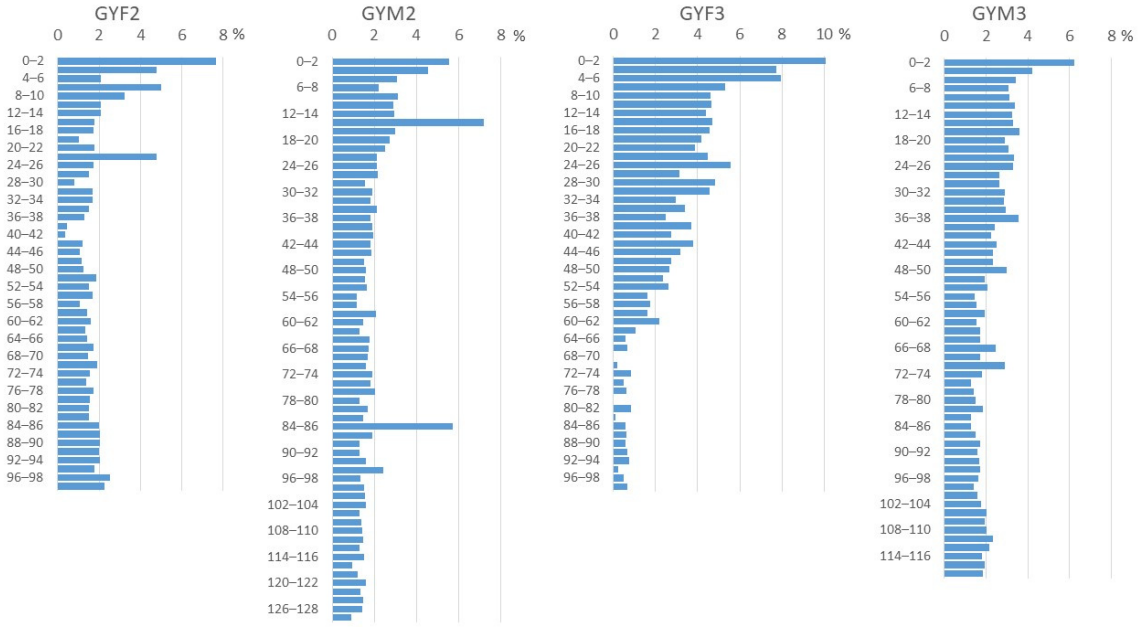

Figure 5. OC content of sediment layers in different floodplain forms.

We also observed significant differences in electrical conductivity (EC) values between natural levees and oxbow lakes (Figure 6). Significantly higher EC values were measured in oxbow lakes. In the GYM2 oxbow lake, the average value was 255 µS/cm, while in the associated natural levee GYF2, we found an average value of only 106 µS/cm. Compared to the average of 202 µS/cm in the old GYM3 oxbow lake, the average EC value in the natural levee (GYF3) was only 102 µS/cm.

Figure 6. EC values of sediment layers in individual floodplain forms.

https://doi.org/10.3390/land15020322

Based on the grain composition of the profiles examined, it can be concluded that the coarsest grain composition characterizes the GYF2 natural levee (Figure 7). Fine grained sand reaches values above 30% in some layers, while the clay fraction is around 10%. The sediments of the GYF3 natural levee are composed of significantly finer grains. The dominant fraction is fine silt, with a proportion exceeding 30% in the lower parts of the profile. The proportion of fine grained sand typically remains below 10%. The GYM2 and GYM3 oxbow lakes show greater vertical variation in sediment composition than the GYF3 levee, which has been inactive for centuries. Here, too, fine silt is the dominant fraction, but the proportion of clay shows much greater vertical variation than in the natural levees. The proportion of small grained sand is the smallest in these profiles.

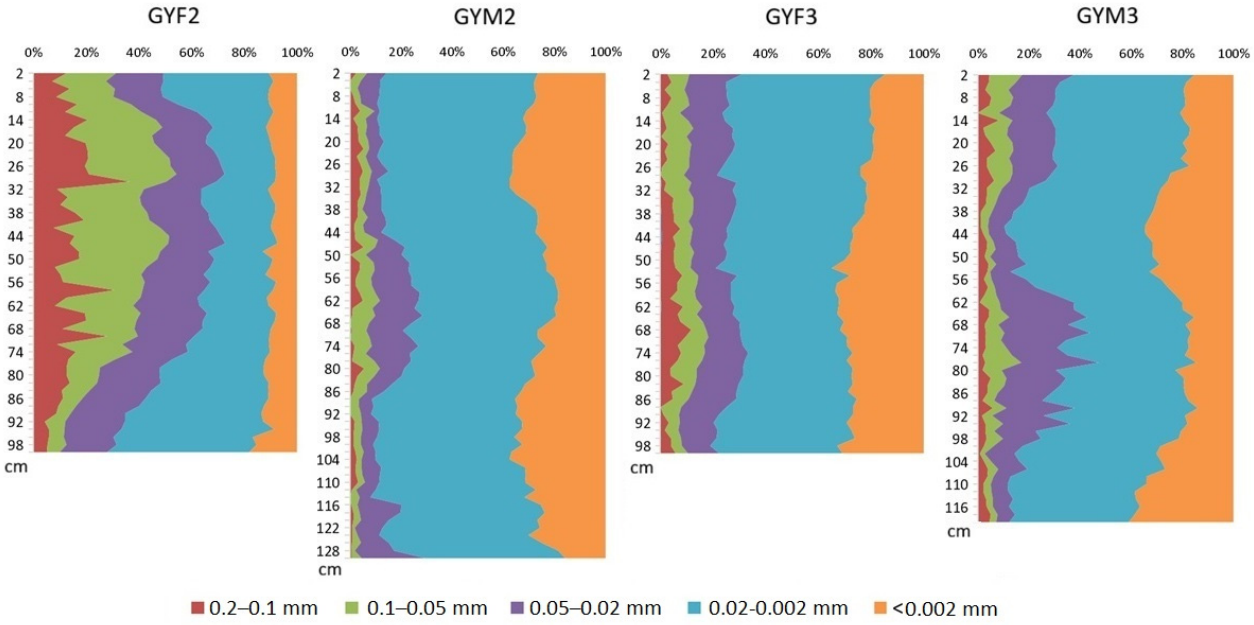

Figure 7. Grain size distribution of sediment layers in individual floodplain forms.

3.3. Statistical Analysis

Within the profiles of individual floodplain forms, we tried to find out whether it is possible to identify layers that were formed under energy conditions and floodplain environments different from the current ones.

The distribution of the samples was analyzed using the Shapiro-Wilk test (Table 2). Since the significance level of the majority of the examined parameters was not higher than 0.05, we concluded that they were not normally distributed, and therefore we calculated Spearman's correlation coefficient during the correlation analysis.

Table 2. Normality test for the examined parameters.

Parameters	Shapiro–Wilk Statistic	df	Sig.
pH (H_2O)	0.902	79	0.000
pH (KCl)	0.929	79	0.000
EC	0.915	79	0.000
$CaCO_3$	0.975	79	0.120
OC	0.875	79	0.000
Small grained sand (0.2–0.1 mm)	0.696	79	0.000
Fine grained sand (0.1–0.05 mm)	0.753	79	0.000
Coarse silt (0.05–0.02 mm)	0.909	79	0.000
Fine silt (0.02–0.002 mm)	0.749	79	0.000
Clay (<0.002 mm)	0.960	79	0.014

3.3.1. Correlation Analysis

We used Spearman's correlation coefficients to examine the relationship between the parameters studied. The correlation matrix is shown in Table 3, in which significant correlations at the 0.01 level are marked with color.

Table 3. Correlation matrix of the parameters examined.

	pH (H_2O)	pH (KCl)	EC	$CaCO_3$	OC	Coarse and Medium Grained sand I (2–0.2 mm)	Small Grained Sand (0.2–0.1 mm)	Fine Grained Sand (0.1–0.05 mm)	Coarse Silt (0.05–0.02 mm)	Fine Silt (0.02–0.002 mm)	Clay (<0.002 mm)
pH (H_2O)	1.00	0.86	0.46	0.13	−0.39	−0.24	−0.49	−0.49	−0.20	0.36	0.34
pH (KCl)	0.86	1.00	0.57	0.31	−0.26	−0.35	−0.37	−0.48	−0.07	0.37	0.11
EC	0.46	0.57	1.00	0.37	0.30	−0.25	−0.53	−0.57	−0.51	0.70	0.38
$CaCO_3$	0.13	0.31	0.37	1.00	−0.09	−0.21	−0.06	−0.17	−0.09	0.20	0.00
OC	−0.39	−0.26	0.30	−0.09	1.00	0.15	−0.12	0.00	−0.15	0.21	0.03
Coarse and medium grained sand (2–0.2 mm)	−0.24	−0.35	−0.25	−0.21	0.15	1.00	0.14	0.06	−0.09	−0.20	0.19
Small grained sand (0.2–0.1 mm)	−0.49	−0.37	−0.53	−0.07	−0.12	0.14	1.00	0.54	0.44	−0.75	−0.48
Fine grained sand (0.1–0.05 mm)	−0.49	−0.42	−0.57	−0.17	0.000	0.06	0.54	1.00	0.72	−0.72	−0.75
Coarse silt (0.05–0.02 mm)	−0.20	−0.07	−0.51	−0.09	−0.15	−0.09	0.44	0.72	1.00	−0.62	−0.88
Fine silt (0.02–0.002 mm)	0.36	0.37	0.70	0.20	0.21	−0.20	−0.75	−0.72	−0.62	1.00	0.46
Clay (<0.002 mm)	0.34	0.11	0.38	0.00	0.03	0.19	−0.48	−0.75	−0.88	0.46	1.000

The colored cells indicate when the correlation is significant at the 0.01 level. (2-tailed).

The chemical effect has a significant correlation with almost all parameters examined at the 0.01 level.

3.3.2. PCA Analysis

While correlation analysis only shows the direction and strength of the relationship between each variable, PCA (Principal Component Analysis) provides much more complex information about the structure and formation of sediment layers, as it reveals multivariate relationships rather than just pairwise relationships, thus examining the common patterns of all variables at once, thereby identifying groups of variables that vary together. PCA is thus able to identify hidden sedimentological patterns and processes that are not apparent from the correlation analysis alone.

During the PCA, we identified five principal components that explain 88.35% of the total variance (Table 4). Five principal components were retained because they cumulatively explained more than 88% of the total variance. According to the Kaiser criterion (eigenvalues >1) and the scree-plot inflection point, the first five components represented statistically and environmentally meaningful structures. Beyond the fifth component, additional axes contributed negligibly to variance explanation and lacked clear geomorphological interpretation. The first two principal components stand out, as they explain 60.64% of the total variance, which is an exceptionally good result for sedimentological databases. This means that the first two principal components (PC1, PC2) together are suitable for the primary interpretation of the main differences between the samples and sections.

Table 4. Total variance explained.

Component	Initial Eigenvalues		
	Total	% of Variance	Cumulative %
1	4.62	42.00	42.00
2	2.05	18.64	60.64
3	1.30	11.84	72.48
4	0.98	8.93	81.41
5	0.76	6.95	88.35

3.3.3. Cluster Analysis

Based on K-means cluster analysis, the 222 sediment samples can be classified into five distinct groups (Table 5). Five clusters were retained based on a marked increase in fusion distance observed when reducing the structure to four clusters. The dendrogram pattern and ANOVA results confirmed the statistical validity of the classification. Furthermore, the identified clusters represent geomorphologically and sedimentologically interpretable floodplain units within the studied profiles. The size and distribution of the clusters are as follows: Cluster 1: 22 samples (9.9%), Cluster 2: 35 samples (15.8%), Cluster 3: 87 samples (39.2%), Cluster 4: 19 samples (8.6%), Cluster 5: 59 samples (26.6%). The Euclidean distances calculated between the centers of the clusters (Table 5) confirm the marked separation of the groups. The smallest distance was observed between clusters 3 and 5 (2.694), while the largest was between clusters 2 and 3 (6.044). The average inter-cluster distance was 4.49, indicating good separation between the groups.

Table 5. Distances between cluster centers.

Distances Between Final Cluster Centers					
Cluster	**1**	**2**	**3**	**4**	**5**
1		5.084	3.955	4.126	3.117
2	5.084		6.044	5.472	4.110
3	3.955	6.044		4.673	2.694
4	4.126	5.472	4.673		3.866
5	3.117	4.110	2.694	3.866	

One-way analysis of variance (ANOVA) showed significant differences between clusters for all variables examined ($p < 0.001$) (Table 6). The F-values were extremely high, indicating strong discrimination between clusters.

Table 6. ANOVA results, differences between clusters.

	Cluster		Error		F	Sig.
	Mean Square	df	Mean Square	df		
pH (H_2O)	30.153	4	0.464	217	64.951	$p < 0.000$
pH (KCl)	26.283	4	0.530	217	49.590	$p < 0.000$
EC	25.275	4	0.549	217	46.063	$p < 0.000$
$CaCO_3$	9.270	4	0.839	217	11.051	$p < 0.000$
OC	30.511	4	0.459	217	66.446	$p < 0.000$
Coarse and medium grained sand (2–0.2 mm)	46.523	4	0.174	217	268.006	$p < 0.000$
Small grained sand (0.2–0.1 mm)	37.481	4	0.334	217	112.101	$p < 0.000$
Fine grained sand (0.1–0.05 mm)	46.258	4	0.177	217	261.097	$p < 0.000$
Coarse silt (0.05–0.02 mm)	32.417	4	0.429	217	75.598	$p < 0.000$
Fine silt (0.02–0.002 mm)	46.345	4	0.168	217	275.327	$p < 0.000$
Clay (<0.002 mm)	36.280	4	0.358	217	101.243	$p < 0.000$

The grain composition variables showed the strongest separation, especially coarse and medium sand, fine sand, and fine silt.

Among the chemical variables, EC, pH (H_2O), pH (KCl) and OC also showed relatively strong separation. The $CaCO_3$ content contributed to the separation of clusters to a much lesser extent, but still significantly (Table 6).

In order to characterize each cluster, we examined the mean and standard deviation values of the parameters belonging to the clusters, which are shown in Table 7.

Table 7. Average values and standard deviations of the parameters examined in each cluster.

Clusters		pH (H_2O)	pH (KCl)	EC	$CaCO_3$	OC	2–0.2 mm	0.2–0.1 mm	0.1–0.05 mm	0.05–0.02 mm	0.02–0.002 mm	<0.002 mm
1	Mean	5.61	4.46	197.2	4.93	5.37	0.00	3.18	9.90	15.65	52.19	19.09
	Std. Dev.	0.37	0.52	114.9	1.52	1.73	0.00	3.03	4.76	3.92	5.40	5.14
2	Std. Dev.	5.67	4.73	84.7	5.87	1.61	0.00	16.25	27.11	21.59	25.50	9.55
	Std. Dev.	0.15	0.34	34.9	0.96	0.75	0.00	6.44	7.20	2.39	4.83	1.40
3	Std. Dev.	7.08	5.90	244.2	6.30	1.96	0.00	2.44	3.84	9.65	54.74	29.33
	Std. Dev.	0.73	0.72	81.3	1.27	0.77	0.00	1.43	1.86	4.51	3.63	5.69
4	Std. Dev.	5.79	4.29	102.8	4.90	2.67	0.32	5.25	7.21	14.09	45.34	27.78
	Std. Dev.	0.29	0.13	15.0	1.05	1.10	0.14	1.90	1.44	1.93	4.13	4.54
5	Std. Dev.	6.54	5.28	138.3	5.11	1.76	0.00	5.09	7.16	19.79	47.70	20.26
	Std. Dev.	0.52	0.72	52.1	1.58	0.94	0.01	3.13	2.45	5.13	5.08	6.05

4. Discussion

4.1. Terrain Interpretation

Based on the data from the terrain model, it can be concluded that the greater difference in level observed at GYM2 is clearly a consequence of the fact that the GYM2 oxbow lake inactivated later, so the accumulation process is less advanced there. This is evidenced by the much greater steepness of the concave bank of the GYM2 oxbow lake (Figure 2). The reason for this is that the erosion processes that have been at work since the backwater oxbow lake came into existence have had less time to exert their effects, so the bank has better retained its original, nearly vertical shape. The studies conducted on the Peruvian section of the Ucayali River have similar results, showing a close correlation between the age of the oxbow lake and the erosion of the banks [49]. Based on the examination of 28 oxbow lakes along the Brazos River in Texas, a similar conclusion was reached: oxbow lakes are more advanced in terms of sedimentation, even if they are located further away from the active channel [50].

4.2. Physicochemical Evaluation of Sediments

The distribution of pH (H_2O) values within the section shows a clear, increasing tendency with depth in the case of sections GYM2, GYM3, and GYF3. This can be partly attributed to the higher OC content of the layers close to the surface. Humic acids cause a decrease in pH. This finding is supported by the significant negative correlation between pH (H_2O) and OC at the 0.01 level. (Table 3). This observation is supported by the works of other authors [9,51].

No significant trends can be observed in the distribution of $CaCO_3$ content within the sections. The younger GYM2 channel and GYF2 natural levee sections have higher $CaCO_3$ content, while the older GYM3 and GYF3 sections have an average $CaCO_3$ content that is 1.5% lower. The reason for this difference is currently unknown and will be the subject of further investigation. $CaCO_3$ shows a significant positive correlation with pH (KCl) and EC at the 0.01 level, which has also been demonstrated in other studies [52], but in our work no significant correlation can generally be detected with the other parameters examined.

With regard to the distribution of OC content within the section, it can be concluded that the amount of OC decreases with depth, but higher values may occur in certain layers, which is characteristic of floodplain sediments [34]. According to some studies, the amount of OC depends on the age of the surface, because older surfaces typically have longer periods of plant cover, allowing more organic matter to form and accumulate [35].

The EC value in oxbow lakes is approximately double that of natural levees. These differences can clearly be attributed to differences in grain composition, as the sediment layers of oxbow lakes have a much finer grain composition and a much higher adsorption capacity, capable of binding many more cations, which explains the higher electrical

conductivity (EC) values. Due to their lower elevation, oxbow lakes are flooded much more frequently, and this reductive, stagnant water condition is fundamentally conducive to the storage of dissolved salts. In contrast, natural levees, especially the GYF2 section, are composed of coarser grained sediments, which allow for faster water permeability, resulting in faster ion leaching.

Based on the grain composition of the sections, it can be concluded that the examined layers of the GYM2 and GYM3 oxbow lakes and the GYF3 natural levee accumulated under low energy conditions due to their high silt and clay content. While a significant part of the GYF2 section layer sequence—between 84 and 16 cm—accumulated under higher energy conditions, as indicated by sediments with a coarser grain composition. The proportions of each fraction are very similar in the GYM3 and GYM2 oxbow lakes (Figure 7).

The 85–90% clayey-silt layer between 120 and 98 cm in the GYM3 oxbow lake is covered by a layer with 35–45% sand content between 98 and 60 cm and it could have accumulated in the active, higher energy condition phase of the GYM2 oxbow lake, before the meander cutoff, i.e., before 1852. Meanwhile, the 60 cm layer above it, which suddenly becomes finer, accumulated after 1852 under much lower energy conditions (Figure 7). Its specific accumulation rate is 0.35 cm/year. Figure 8 shows the changes in the course of the Tisza River from 1852 to the present day. The 1976 course is almost identical to the current one. In the case of the GYM2 sediment section, we have not yet reached the sand deposit marking the bottom of the riverbed at 130 cm (Figure 7), so the entire layer was deposited after 1852. Thus, although we cannot specify the actual accumulating rate, it cannot be less than 0.76 cm/year. In the section approximately 10–20 km upstream from our study area, an annual sedimentation rate of 0.9–1.3 cm was observed in the oxbow lakes [1,29,43] Balogh et al. [53] measured an accumulation of at least 1 cm/year in the Middle Tisza region for oxbow lakes of similar age. On the Hungarian section of the Maros River, which has very similar hydrological characteristics to the Upper Tisza, the rate of accumulation of oxbow lakes in the floodplain is 1.3–2.4 cm/y [40], which is of the same order of magnitude as that observed on the Upper Tisza.

The same can be stated about data measured in similar sections of other European rivers. Along the Aare and Rhine rivers, values of 0.4–1.8 cm/year were measured [54], while in the Eastern European Plain, the rate of sedimentation was slightly lower, between 0.2 and 0.6 cm/year [12].

Giardino and Lee [52] found similar results along the Brazos River in Texas, where they found that younger oxbow lakes closer to the active channel had faster accumulation rates, up to 4 cm/year, than more distant, typically older oxbow lakes, where the minimum accumulation rate was 0.27 cm/year.

Despite the fact that GYF3 is a natural levee area, its development as an active natural levee ceased centuries ago, so sediment layers with a much finer grain composition were deposited on its surface, which indicates a distal floodplain condition.

In the GYF2 natural levee section, between 100 and 16 cm, there is a coarser sediment profile characteristic of active natural levee. The formation of recent natural levees observed along the Tisza River can reach up to 10 cm during certain floods [55]. Thus, this layer could have accumulated relatively quickly. The 16 cm layer above it consists of much finer grains. This can be explained by the sudden decrease in energy conditions following the cutoff the meander in 1852. Based on this, we can calculate an average accumulation rate of 0.1 cm/year for the 171 years between the cutting off of the meander and the sampling.

Accumulation values of this magnitude can be observed in the highest forms in relation to the entire floodplain. Károlyi [56] examined, among other things, whether there is a correlation between the width of the floodplain and the rate of sediment accumulation along the entire Hungarian section of the Tisza. He found that in the case of narrow floodplains (250–500 m),

the average accumulation rate is 0.6–1.3 cm/year, while in the case of wide floodplains (500–3500 m), this value is lower, at 0.1–0.4 cm/year. Gábris and colleagues [38], who also studied the accumulation of the entire floodplain several kilometers wide in the Middle Tisza region using DTM, measured a similar specific accumulation rate. Since our sample area is of similar width, the accumulation of its entire area may also be of a similar magnitude.

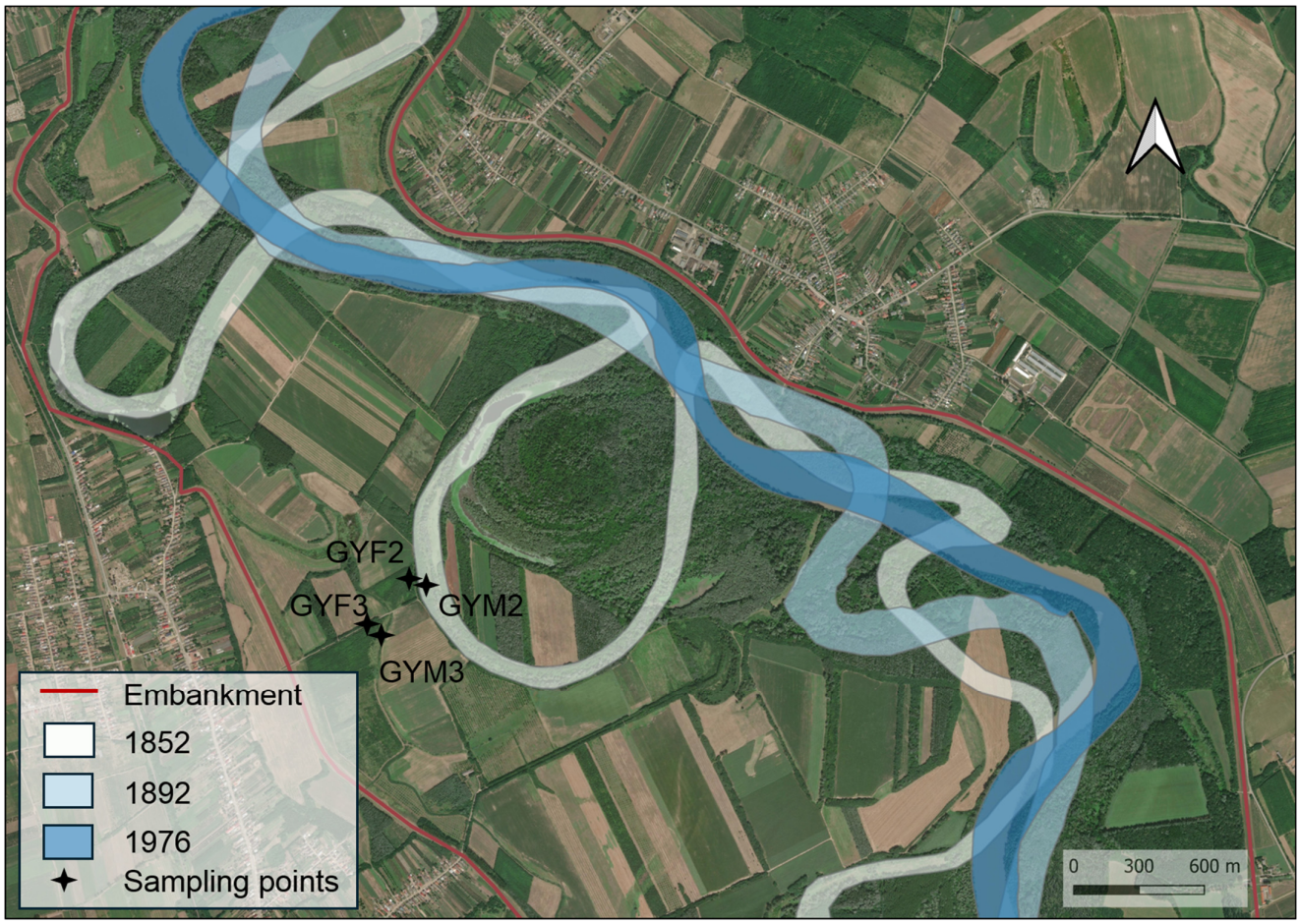

Figure 8. Changes in the course of the Tisza River between 1852 and 1976. Base map: Bing Satellite Imagery © Microsoft (Washington, DC, USA).

4.3. Evaluation of Statistical Analyses

Using Spearman's correlation analysis, a strong correlation was found, significant at the 0.01 level, between the pH and most of the parameters examined. The relationship is positive with electrical conductivity, as higher EC values indicate higher dissolved ion content, which in the sediments of the Tisza floodplain are mostly HCO_3^-, Ca^{2+}, and Mg^{2+} ions, resulting in an alkaline chemical effect [57,58]. There is also a positive correlation with fine grain fractions, as this fraction has a much better cation binding capacity, while a negative correlation can be observed with coarser grain fractions of the sediment [59]. The correlation with OC content is also negative, which is due to the fact that organic acids are produced during the decomposition of organic matter, which have an acidifying effect, so the pH is typically lower in sections with higher OC content. This correlation is particularly noticeable in the upper layers of oxbow lakes, where higher OC content, even above 6%, is associated with lower pH values (Figures 3 and 5). In the upper 30 cm layer of the GYM2 section, pH values below 6 were measured throughout, while in the lower layers of the section, the pH rose to around 7.5–8, generally with an OC content well below 2%.

During PCA analysis, we identified five principal components, of which the first two explain more than 60% of the total variance. (Table 4). The first principal component in the case of grain composition illustrates the gradient formed along the fine and coarse grain fractions, which is closely related to the hydrodynamic energy state (Figure 9). The PC1 axis represents a clear texture gradient. Negative PC1 values are associated with fine grained fractions (clay and fine silt) and higher electrical conductivity (EC), which are typical of oxbow and low energy floodplain deposits. In contrast, positive PC1 values correspond to coarser, sand-rich sediments, mainly occurring on natural levees, including the GYF2 section. PC1 explains 42% of the total variance.

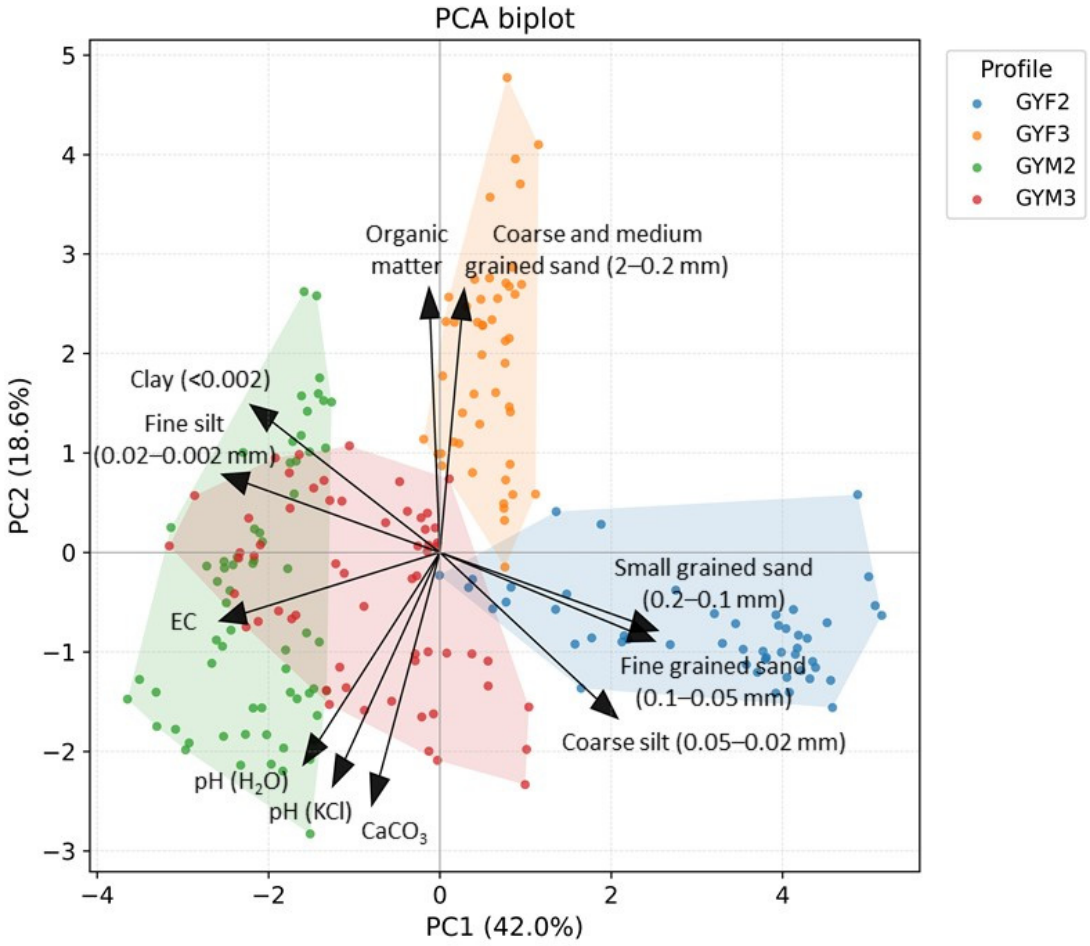

Figure 9. Separation of sedimentation environments in the PC1–PC2 space.

The PC2 axis reflects a chemical-organic matter gradient. Negative PC2 values are related to higher pH and $CaCO_3$ content, indicating more alkaline, carbonate rich sediments, whereas positive PC2 values are associated with higher organic carbon (OC) content. Thus, PC2 distinguishes carbonate rich, alkaline deposits from organic matter rich surface layers of the floodplain.

The sediment profile established on the two natural levees is clearly separated from the two oxbow lakes, primarily along the first principal component. At the same time, the natural levees are also separated along the first principal component, as the proportion of fine grain fractions is significantly higher in the GYF3 natural levee section than in the GYF2 section. Most of the samples from the oxbow lakes fall within the negative range of the first principal component, with a relatively large overlap between the two sections, mainly due to the higher pH values of the samples, which are mostly in the alkaline range.

The exception is the sediment layers of the GYM2 section, which are rich in OC, acidic, and fall within the pH range of 5 to 6.

We were able to correspond each of the five clusters obtained during the cluster analysis to a characteristic floodplain environment. (Figure 10).

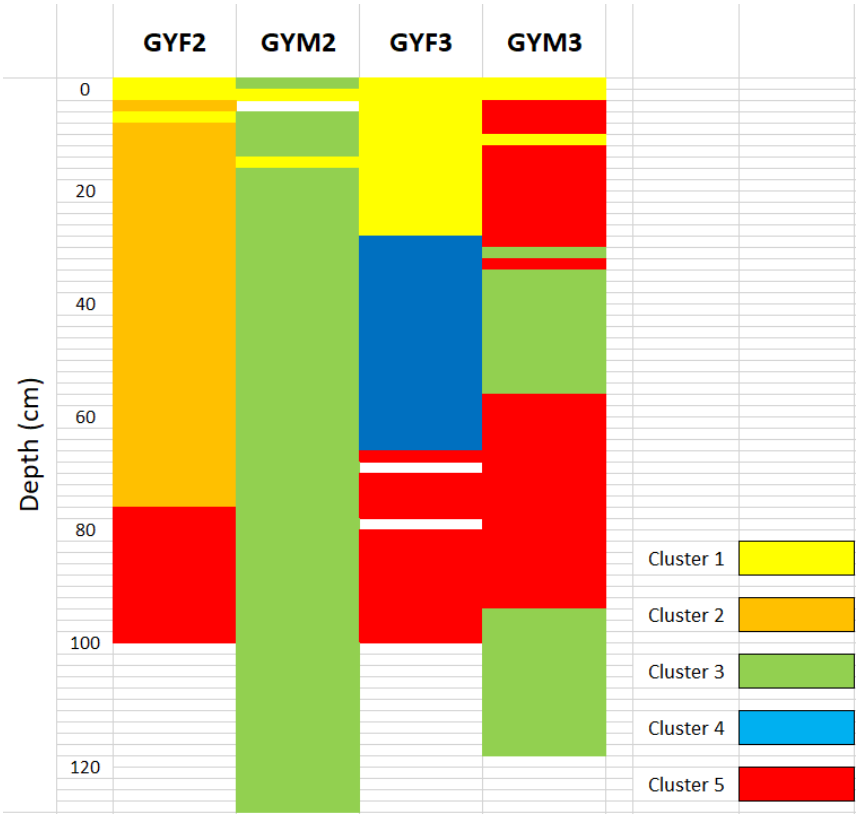

Figure 10. Appearance of each cluster in the sections examined.

Cluster 1: Low energy environment with soil formation processes (N = 22).

This cluster describes fine grained, silty-clayey layers rich in OC, with a slightly acidic pH and relatively high EC. This type appears in the surface or near-surface layers of each section and has characteristics typical of soil level "A," suggesting that soil formation processes have begun in the surface sediment layers covered with vegetation, which is consistent with OC accumulation (Figure 10).

Cluster 2: Active riverine environment characterized by higher energy levels and increased accumulation (N = 35).

This cluster represents a coarser, sandy, coarse silty sediment type with good water permeability and low OC content, in which the carbonate component is significant but the dissolved salt content (EC) is low. From a sedimentological point of view, it is a characteristic type of higher energy natural levee sediment (Figure 10).

Cluster 3: Low energy oxbow lake environment (N = 87).

The samples in the third cluster are dominated by clay and silt fractions, slightly alkaline and rich in salts, with a significant amount of carbonate. This type is characteristic of stagnant water, deeper lying areas covered with water for long periods of time (Figure 10).

Cluster 4: Low energy fossil natural levee environment (N = 19).

This cluster refers to layers with a fine silty-clay texture, slightly acidic, occasionally neutral chemical properties, and moderate OC and salt content. Based on its properties,

it occupies an intermediate position between the OC-richer, near-surface, soil-like layers (cluster 1) and the deeper, more alkaline, salt-rich sediment layers (cluster 3) (Figure 10).

Cluster 5: Medium energy environment (N = 59).

The fifth cluster represents a moderately fine, typically silty-clayey, moderately carbonate-rich, OC-poor sediment type, with a slightly acidic, occasionally neutral pH and medium EC. The OC content of these fine sediment layers is lower than that of cluster 1, and their pH and electrical conductivity are lower than those of cluster 3 (Figure 10). These parameters suggest a relatively common environment for an oxbow lake, from which larger amounts of coarse grained silt arrived from time to time (Figures 7 and 10).

In the natural levees sections (GYF2, GYF3), the cluster profiles clearly show the OC-rich surface zone formed by soil formation (cluster 1), with coarser natural levee sediment layers (cluster 2, only GYF2) and fine floodplain sediments (clusters 4 and 5) underneath (Figures 5 and 10).

In contrast, in the oxbow lake sections (GYM2, GYM3), the dominance of cluster 3 indicates a slightly alkaline, fine grained, high EC, carbonate oxbow lake accumulation, which is divided by thin, discontinuous OC (cluster 1) and transitional fine sediment (cluster 5) layers (Figures 6 and 10).

5. Conclusions

Our study provides a comprehensive assessment of the development of the Upper Tisza active floodplain following river regulation. By integrating topographic assessment with high-resolution sedimentological and statistical analyses, we have successfully reconstructed the different surface development conditions of the individual floodplain forms.

During the topographic assessment, we found that there is a close relationship between the age and morphology of oxbow lakes. In older oxbow lakes with more advanced accumulation, the slope of the concave side wall is much smaller, in contrast to younger, less accumulated oxbow lakes that better preserve the original shape of the bank. We confirmed that the development of the oxbow lakes took place under low energy conditions, which favored the accumulation of fine grained, carbonate-rich sediments with higher electrical conductivity. The development of natural levees took place in a higher energy environment, resulting in sediments with a coarser structure, better water permeability, and greater leaching. We successfully identified the sharp imprint of river regulation in the stratigraphic sequences, indicated by the sudden change from sandy sediments to silty-clayey sediments. This precisely marks the 1852 meander cut. With this, we determined that the sedimentation rate for older oxbow lakes is 0.34 cm/year, while for younger ones it is at least 0.76 cm/year, which is much higher than the 0.1 cm/year sedimentation rate for younger natural levee. These results support the role of oxbow lakes as sediment traps. Using PCA, we were able to demonstrate that, in addition to morphological differences, there are also clear differences in the physical and chemical properties of sediments in oxbow lakes and natural levees. Cluster analysis identified five different floodplain environments, whose vertical location determined the surface development of individual form. Statistical processing of the sedimentological results enabled us to perform a more accurate surface development reconstruction. The research goals were achieved with the applied methods, but there is no doubt that the inclusion of other methods can contribute to a more accurate understanding of the processes of the floodplain environment. These methods include the measurement of 137C and 210Pb activity, and the identification of heavy metal profiles, the application of which is among our future goals.

Author Contributions: Conceptualization, R.V. and G.S.; methodology, R.V. and G.S.; software, R.V., A.R. and G.S.; formal analysis, R.V. and G.S.; investigation, R.V., A.R., P.C., D.B., B.B. and G.S.; resources, R.V. and G.S.; data curation, R.V., A.R. and G.S.; writing—original draft preparation, R.V. A.R., P.C., D.B., B.B. and G.S.; writing—review and editing, R.V. A.R., P.C., D.B., B.B. and G.S.; visualization, R.V., A.R. and G.S.; supervision, R.V., A.R. and G.S. All authors have read and agreed to the published version of the manuscript.

Funding: Supported by the University of Debrecen Scientific Research Bridging Fund (DETKA). Project no. TKP2021-NKTA-32 has been implemented with the support provided from the National Research, Development and Innovation Fund of Hungary, financed under the TKP2021-NKTA funding scheme.

Data Availability Statement: The data presented in this study are available on request from the corresponding author.

Conflicts of Interest: The authors declare no conflicts of interest.

References

1. Vass, R.; Szabó, G.; Szabó, J. Examination of Sedimentary Deposition in the Active Floodplains of Bereg-Plain. *Stud Univ "Vasile Goldiş" Ser Ştiinţ Vieţii.* **2010**, *20*, 105–110.
2. Sándor, A. A Hullámtér-Feltöltődés Folyamatának Vizsgálata a Tisza Középső és Alsó Szakaszán. Ph.D Thesis, Szegedi Tudományegyetem, Szeged, Hungary, 2012; p. 1084. Available online: http://doktori.bibl.u-szeged.hu/1084/ (accessed on 28 September 2025).
3. Kiss, T.; Sipos, G.; Vass, R. Alluvial Ridge Development and Structure: Case study on the Upper Tisza, Hungary. *Geogr. Pannonica* **2022**, *26*, 230–240. [CrossRef]
4. Molnár, G.; Scholtz, A.; Vass, R. Accumulation studies at specific sampling areas of the active floodplain in the Upper-Tisza region. *ACTA Geogr Debrecina Landsc Environ.* **2017**, *11*, 14–22. [CrossRef]
5. Konecsny, K. A Felső-Tisza 1998-2001. évi árvizeinek hidrológiai értékelése. *Hidrol. Közlöny* **2003**, *83*, 75–85.
6. Szczepańska, A.; Zaborska, A.; Pempkowiak, J. Sediment Accumulation Rates in the Gotland Deep, Baltic Proper Obtained by 210Pb and 137Cs Methods. *Rocz. Ochr. Sr.* **2009**, *11*, 77–85.
7. Humphries, M.S.; Kindness, A.; Ellery, W.N.; Hughes, J.C.; Benitez-Nelson, C.R. 137Cs and 210Pb derived sediment accumulation rates and their role in the long-term development of the Mkuze River floodplain, South Africa. *Geomorphology* **2010**, *119*, 88–96. [CrossRef]
8. Yoshimura, K.; Onda, Y.; Fukushima, T. Sediment particle size and initial radiocesium accumulation in ponds following the Fukushima DNPP accident. *Sci. Rep.* **2014**, *4*, 4514. [CrossRef]
9. Scott, D.N.; Wohl, E.E. Geomorphic regulation of floodplain soil organic carbon concentration in watersheds of the Rocky and Cascade Mountains, USA. *Earth Surf. Dyn.* **2018**, *6*, 1101–1114. [CrossRef]
10. Vinichuk, M.; Simonsson, M.; Larsson, M.; Rosén, K. Long-term transfer of 137Cs in sensitive agricultural environments after the Chornobyl fallout in Sweden. *J. Environ. Radioact.* **2025**, *282*, 107621. [CrossRef]
11. Hughes, A.O.; Olley, J.M.; Croke, J.C.; Webster, I.T. Determining floodplain sedimentation rates using 137Cs in a low fallout environment dominated by channel- and cultivation-derived sediment inputs, central Queensland, Australia. *J. Environ. Radioact.* **2009**, *100*, 858–865. [CrossRef]
12. Golosov, V.N.; Belyaev, V.R.; Markelov, M.V. Application of Chernobyl-derived 137Cs fallout for sediment redistribution studies: Lessons from European Russia. *Hydrol. Process.* **2013**, *27*, 781–794. [CrossRef]
13. Golosov, V.; Walling, D.E. Using fallout radionuclides to investigate recent overbank sedimentation rates on river floodplains: An overview. *Proc. Int. Assoc. Hydrol. Sci.* **2015**, *367*, 228–234. [CrossRef]
14. Chen, X.; Qiao, Q.; McGowan, S.; Zeng, L.; Stevenson, M.A.; Xu, L.; Huang, C.; Liang, J.; Cao, Y. Determination of geochronology and sedimentation rates of shallow lakes in the middle Yangtze reaches using 210Pb, 137Cs and spheroidal carbonaceous particles. *CATENA* **2019**, *174*, 546–556. [CrossRef]
15. Liu, B.; Wang, Z.; Zhang, X.; Xie, G.; Yin, B.; Liu, G.; Zhang, T. Application of 137Cs tracer technique in floodplain deposition research in mesoscale river basins. *Geoderma* **2023**, *439*, 116706. [CrossRef]
16. Kachanoski, R.G. Comparison of Measured Soil 137-Cesium Losses and Erosion Rates. *Can. J. Soil Sci.* **1987**, *67*, 199–203. [CrossRef]
17. Porto, P.; Walling, D.E.; Callegari, G. Using^{137} Cs measurements to establish catchment sediment budgets and explore scale effects. *Hydrol. Process.* **2011**, *25*, 886–900. [CrossRef]

18. Fulajtár, E.; Mabit, L.; Renschler, C.S.; Yi, A.L.Z. *Use of ^{137}Cs for Soil Erosion Assessment*; Food and Agriculture Organization of the United Nations; International Atomic Energy Agency: Rome, Italy, 2017.
19. Polyakov, V.O.; Nichols, M.N.; Nearing, M.A. Determining soil erosion rates on semi-arid watersheds using radioisotope-derived sedimentation chronology. *Earth Surf. Process. Landf.* **2017**, *42*, 987–993. [CrossRef]
20. Porto, P.; Callegari, G.; Ouadja, A.; Infusino, E. Using Cs-137 measurements and RUSLE model to explore the effect of land use changes on soil erosion and deposition rates in a mid-sized catchment in southern Italy. *Int. J. Sediment Res.* **2023**, *39*, 167–177. [CrossRef]
21. Taylor, M.P. The variability of heavy metals in floodplain sediments: A case study from mid Wales. *CATENA* **1996**, *28*, 71–87. [CrossRef]
22. Graf, J.; Webb, R.; Hereford, R. Relation of sediment load and flood-plain formation to climatic variability, Paria River drainage basin, Utah and Arizona. *Geol. Soc. Am. Bull.* **1991**, *103*, 1405–1415. [CrossRef]
23. Martin, C.W. Heavy metal trends in floodplain sediments and valley fill, River Lahn, Germany. *CATENA* **2000**, *39*, 53–68. [CrossRef]
24. Knox, J.C. Floodplain sedimentation in the Upper Mississippi Valley: Natural versus human accelerated. *Geomorphology* **2006**, *79*, 286–310. [CrossRef]
25. Braun, M.; Szalóki, I.; Posta, J.; Dezső, Z. Üledék-felhalmozódás sebességének becslése a Tisza hullámterében. In Proceedings of the MHT XXI. Vándorgyűlés, Szolnok, Hungary, 2–4 July 2003.
26. Papp, G.; Péter, G.; Halasi-Kovács, B. A halközösség struktúrájának sajátosságai a Tiszató különböző élőhelyein. The attribution of the fish community structure in the different habitat types of the Tiszalake. *Pisces Hung.* **2014**, *8*, 51–60.
27. Szalai, Z.; Baloghné di Gléria, M.; Jakab, G.; Csuták, M.; Tóth, A. A folyópartok alakjának szerepe a hullámtereken kiülepedő üledék szemcse-és nehézfém frakcionációjában, a Duna és a Tisza példáján. *Földrajzi Ért.* **2005**, *54*, 61–84.
28. Sándor, A.; Kiss, T. A területhasználat változás hatása az üledék-felhalmozódásra, közép-tiszai vizsgálatok alapján. In Proceedings of the IV. Magyar Földrajzi Konferencia, Debrecen, Hungary, 14–15 November 2008; pp. 1–6.
29. Szabó, J.; Tóth, C.; Vass, R. Examination of fluvial development on study areas of Upper-Tisza region. *Carpathian J. Earth Environ. Sci.* **2012**, *7*, 241–253.
30. Walling, D.E.; He, Q. The spatial variability of overbank sedimentation on river floodplains. *Geomorphology* **1998**, *24*, 209–223. [CrossRef]
31. Kiss, T.; Nagy, J.; Fehérvári, I.; Amissah, G.J.; Fiala, K.; Sipos, G. Increased flood height driven by local factors on a regulated river with a confined floodplain, Lower Tisza, Hungary. *Geomorphology* **2021**, *389*, 107858. [CrossRef]
32. Magilligan, F.J. Sedimentology of a fine-grained aggrading floodplain. *Geomorphology* **1992**, *4*, 393–408. [CrossRef]
33. Lecce, S.A.; Pavlowsky, R.T. Spatial and temporal variations in the grain-size characteristics of historical flood plain deposits, Blue River, Wisconsin, USA. *Geomorphology* **2004**, *61*, 361–371. [CrossRef]
34. Omengo, F.O.; Geeraert, N.; Bouillon, S.; Govers, G. Deposition and fate of organic carbon in floodplains along a tropical semiarid lowland river (Tana River, Kenya). *J. Geophys. Res. Biogeosci.* **2016**, *121*, 1131–1143. [CrossRef]
35. Lininger, K.B.; Wohl, E.; Rose, J.R. Geomorphic Controls on Floodplain Soil Organic Carbon in the Yukon Flats, Interior Alaska, From Reach to River Basin Scales. *Water Resour. Res.* **2018**, *54*, 1934–1951. [CrossRef]
36. Guo, Y.; Wang, X.; Li, X.; Wang, J.; Xu, M.; Li, D. Dynamics of soil organic and inorganic carbon in the cropland of upper Yellow River Delta, China. *Sci. Rep.* **2016**, *6*, 36105. [CrossRef] [PubMed]
37. Baldwin, D.S.; Paul, W.L.; Wilson, J.S.; Pitman, T.; Rees, G.N.; Klein, A.R. Changes in soil carbon in response to flooding of the floodplain of a semi-arid lowland river. *Freshw. Sci.* **2015**, *34*, 431–439. [CrossRef]
38. Gábris, G.; Telebisz, T.; Nagy, B.; Belardinelli, E. A tiszai hullámtér feltöltődésének kérdése és az üledékképződés geomorfológiai alapjai. *Vízügyi Közlemények* **2002**, *LXXXIV. évfolyam*, 305–316.
39. Vass, R.; Szabó, G.; Szabó, J. Hullámtéri feltöltõdés vizsgálata geoinformatikai módszerekkel a Felsõ-Tisza vidékén. In *Geoinformatika és Domborzatmodellezés*; Miskolci Egyetem: Miskolc, Hungary, 2009; pp. 1–10. Available online: http://www.termeszetfoldrajz.uni-miskolc.hu/Hundem_es_Geoinfo_2009/Cikkek/VassR_SzaboG_SzaboJ.pdf (accessed on 5 November 2025).
40. Kiss, T.; Oroszi, V.G.; Sipos, G.; Fiala, K.; Benyhe, B. Accelerated overbank accumulation after nineteenth century river regulation works: A case study on the Maros River, Hungary. *Geomorphology* **2011**, *135*, 191–202. [CrossRef]
41. Országos Vízügyi Főigazgatóság. Available online: https://www.vizugy.hu/ (accessed on 7 December 2025).
42. Lászlóffy, W. *A Tisza*; Akadémiai Kiadó: Budapest, Hungary, 1982.
43. Vass, R. *Ártérfejlődési Vizsgálatok Felső-Tiszai Mintaterületeken*; Vass Róbert: Nyíregyháza, Hungary, 2018.
44. *Vízrajzi Atlasz Sorozat*; Vízgazdálkodási Tudományos Kutató Központ: Budapest, Hungary, 1979.
45. *A Talaj Fizikai és Vízgazdálkodási Tulajdonságainak Vizsgálata*; Magyar Szabványügyi Testület: Budapest, Hungary, 1978.
46. *A Talaj Egyes Kémiai Tulajdonságainak Vizsgálata. Laboratóriumi Vizsgálatok (pH-Érték, Szódában Kifejezett Fenolftalein Lúgosság, Vízben Oldható Összes só, Hidrolitos/y1-Érték/és Kicserélődési Aciditás/y2-Érték/)*; Magyar Szabványügyi Testület: Budapest, Hungary, 1978.

47. Környezetvédelmi talajvizsgálatok. In *Talajminta Előkészítése, Nedvességtartalom, Elektromos Vezetőképesség és pH Meghatározása*; Magyar Szabványügyi Testület: Budapest, Hungary, 1981.
48. *Talajok Szerves Széntartalmának Elemzése*; Magyar Szabványügyi Testület: Budapest, Hungary, 1977.
49. Li, Z.; Mendoza, A.; Abad, J.D.; Endreny, T.A.; Han, B.; Carrisoza, E.; Dominguez, R. High-resolution modeling of meander neck cutoffs: Laboratory and field scales. *Front. Earth Sci.* **2023**, *11*, 1208782. [CrossRef]
50. Giardino, J.R.; Lee, A.A. Evolution of Oxbow Lakes Along the Brazos River. Department of Geology & Geophysics Texas A&M University: College Station, TX, USA, 2012; p. 33. Available online: https://www.twdb.texas.gov/publications/reports/contracted_reports/doc/0904830969_Brazos_Oxbow.pdf (accessed on 28 January 2026).
51. Shen, Z.; Han, T.; Huang, J.; Li, J.; Daba, N.A.; Gilbert, N.; Khan, M.N.; Shah, A.; Zhang, H. Soil organic carbon regulation by pH in acidic red soil subjected to long-term liming and straw incorporation. *J. Environ. Manag.* **2024**, *367*, 122063. [CrossRef]
52. Shivsagar, V.; Basumatary, D.; Goswami, C.; Rawat, M.; Singh, S.; Jaiswal, M.K. An assessment of oxbow lakes and their potential in reconstructing past river discharge: Implication to reconstruct past climate in Southern West Bengal. *Geochronometria* **2024**, *51*, 192455. [CrossRef]
53. Balogh, J.; Nagy, I.; Schweitzer, F. A Közép-Tisza mente geomorfológiai adottságainak és a hullámterek feliszapolódásának vizsgálata mintaterületeken. *Földrajzi Ért.* **2005**, *54*, 29–59.
54. Eyrolle, F.; Chaboche, P.-A.; Lepage, H.; Gouin, V.N.; Boyer, P.; De Vismes, A.; Seignemartin, G.; Badariotti, D.; Chabaux, F.; Chastanet, M.; et al. Temporal trajectories of artificial radiocaesium 137Cs in French rivers over the nuclear era reconstructed from sediment cores. *Sci. Rep.* **2024**, *14*, 14213. [CrossRef]
55. Schweitzer, F.; Nagy, I.; Alföldi, L. Jelenkori övzátony (parti gát) képződés és hullámtéri lerakódás a Közép-Tisza térségében. *Földrajzi Ért.* **2002**, *51*, 257–278.
56. Károlyi, Z. *A Tisza Mederváltozásai, Különös Tekintettel az Árvízvédelemre*; Tanulmányok és kutatási eredmények; Vízgazdálkodási Tudományos Kutató Intézet: Budapest, Hungary, 1960; p. 102.
57. Khilchevskyi, V.K.; Leta, V.V.; Sherstyuk, N.P.; Pylypovych, O.V.; Zabokrytska, M.R.; Pasichnyk, M.P.; Tsvietaieva, O.V. Hydrochemical characteristics of the Upper reaches of the Tisza River. *J Geol Geogr Geoecology* **2023**, *32*, 283–294. [CrossRef]
58. Flores, Y.G.; Eid, M.H.; Szűcs, P.; Szőcs, T.; Fancsik, T.; Szanyi, J.; Kovács, B.; Markos, G.; Újlaki, P.; Tóth, P.; et al. Integration of Geological, Geochemical Modelling and Hydrodynamic Condition for Understanding the Geometry and Flow Pattern of the Aquifer System, Southern Nyírség–Hajdúság, Hungary. *Water* **2023**, *15*, 2888. [CrossRef]
59. Khan, M.H.R.; Liu, J.; Huang, Y.; Wan, S.; Chen, Z.; Rahman, A. The influence of grain size and mineralogical composition of terrestrial material inputs on organic carbon sequestration in the Bengal Fan since the last deglaciation. *Glob Planet Change* **2025**, *248*, 104773. [CrossRef]